

Search for CP Violation in $D^0 \rightarrow \pi^0 \pi^0$ Decays

N. K. Nisar,⁵² K. Trabelsi,¹⁰ G. B. Mohanty,⁵² T. Aziz,⁵² A. Abdesselam,⁵¹ I. Adachi,¹⁰ H. Aihara,⁵⁷ K. Arinstein,³ D. M. Asner,⁴³ V. Aulchenko,³ T. Aushev,¹⁹ R. Ayad,⁵¹ S. Bahinipati,¹² A. M. Bakich,⁵⁰ A. Bala,⁴⁴ V. Bansal,⁴³ P. Behera,¹⁴ K. Belous,¹⁷ V. Bhardwaj,³⁶ A. Bobrov,³ G. Bonvicini,⁶² A. Bozek,³⁸ M. Bračko,^{29,20} T. E. Browder,⁹ D. Červenkov,⁴ B. G. Cheon,⁸ K. Chilikin,¹⁹ K. Cho,²⁴ V. Chobanova,³⁰ Y. Choi,⁴⁹ D. Cinabro,⁶² J. Dalseno,^{30,53} M. Danilov,^{19,32} Z. Doležal,⁴ Z. Drásal,⁴ A. Drutskey,^{19,32} D. Dutta,¹³ K. Dutta,¹³ S. Eidelman,³ D. Epifanov,⁵⁷ H. Farhat,⁶² J. E. Fast,⁴³ T. Ferber,⁶ V. Gaur,⁵² N. Gabyshev,³ S. Ganguly,⁶² A. Garmash,³ Y. M. Goh,⁸ B. Golob,^{28,20} T. Hara,¹⁰ H. Hayashii,³⁶ X. H. He,⁴⁵ Y. Hoshi,⁵⁵ W.-S. Hou,³⁷ T. Iijima,^{35,34} A. Ishikawa,⁵⁶ R. Itoh,¹⁰ Y. Iwasaki,¹⁰ T. Iwashita,²³ J. H. Kang,⁶⁴ T. Kawasaki,⁴⁰ C. Kiesling,³⁰ D. Y. Kim,⁴⁸ J. B. Kim,²⁵ J. H. Kim,²⁴ M. J. Kim,²⁶ Y. J. Kim,²⁴ K. Kinoshita,⁵ B. R. Ko,²⁵ P. Kodyš,⁴ S. Korpar,^{29,20} P. Križan,^{28,20} P. Krokovny,³ T. Kuhr,²² R. Kumar,⁴⁶ A. Kuzmin,³ Y.-J. Kwon,⁶⁴ J. S. Lange,⁷ S.-H. Lee,²⁵ L. Li Gioi,³⁰ J. Libby,¹⁴ D. Liventsev,¹⁰ P. Lukin,³ B. Macek,⁹ D. Matvienko,³ K. Miyabayashi,³⁶ H. Miyata,⁴⁰ R. Mizuk,^{19,32} A. Moll,^{30,53} R. Mussa,¹⁸ E. Nakano,⁴² M. Nakao,¹⁰ M. Nayak,¹⁴ E. Nedelkovska,³⁰ O. Nitoh,⁶⁰ S. Ogawa,⁵⁴ S. Okuno,²¹ P. Pakhlov,^{19,32} G. Pakhlova,¹⁹ H. Park,²⁶ H. K. Park,²⁶ T. K. Pedlar,⁶⁵ T. Peng,⁴⁷ R. Pestotnik,²⁰ M. Petrič,²⁰ L. E. Piilonen,⁶¹ E. Ribežl,²⁰ M. Ritter,³⁰ M. Röhrken,²² A. Rostomyan,⁶ Y. Sakai,¹⁰ S. Sandilya,⁵² L. Santelj,²⁰ T. Sanuki,⁵⁶ Y. Sato,⁵⁶ O. Schneider,²⁷ G. Schnell,^{1,11} C. Schwanda,¹⁶ A. J. Schwartz,⁵ D. Semmler,⁷ K. Senyo,⁶³ O. Seon,³⁴ M. E. Sevier,³¹ M. Shapkin,¹⁷ V. Shebalin,³ T.-A. Shibata,⁵⁸ J.-G. Shiu,³⁷ B. Shwartz,³ F. Simon,^{30,53} Y.-S. Sohn,⁶⁴ A. Sokolov,¹⁷ E. Solovieva,¹⁹ S. Stanič,⁴¹ M. Starič,²⁰ M. Steder,⁶ J. Stypula,³⁸ T. Sumiyoshi,⁵⁹ G. Tatishvili,⁴³ Y. Teramoto,⁴² M. Uchida,⁵⁸ T. Uglov,^{19,33} S. Uno,¹⁰ P. Urquijo,² Y. Usov,³ S. E. Vahsen,⁹ C. Van Hulse,¹ P. Vanhoefer,³⁰ G. Varner,⁹ K. E. Varvell,⁵⁰ M. N. Wagner,⁷ C. H. Wang,⁶⁶ M.-Z. Wang,³⁷ P. Wang,¹⁵ Y. Watanabe,²¹ K. M. Williams,⁶¹ E. Won,²⁵ J. Yamaoka,⁴³ Y. Yamashita,³⁹ S. Yashchenko,⁶ Y. Yook,⁶⁴ Z. P. Zhang,⁴⁷ V. Zhilich,³ V. Zhulanov,³ and A. Zupanc²⁰

(Belle Collaboration)

¹University of the Basque Country UPV/EHU, 48080 Bilbao²University of Bonn, 53115 Bonn³Budker Institute of Nuclear Physics SB RAS and Novosibirsk State University, Novosibirsk 630090⁴Faculty of Mathematics and Physics, Charles University, 121 16 Prague⁵University of Cincinnati, Cincinnati, Ohio 45221⁶Deutsches Elektronen-Synchrotron, 22607 Hamburg⁷Justus-Liebig-Universität Gießen, 35392 Gießen⁸Hanyang University, Seoul 133-791⁹University of Hawaii, Honolulu, Hawaii 96822¹⁰High Energy Accelerator Research Organization (KEK), Tsukuba 305-0801¹¹IKERBASQUE, Basque Foundation for Science, 48011 Bilbao¹²Indian Institute of Technology Bhubaneswar, Satya Nagar 751007¹³Indian Institute of Technology Guwahati, Assam 781039¹⁴Indian Institute of Technology Madras, Chennai 600036¹⁵Institute of High Energy Physics, Chinese Academy of Sciences, Beijing 100049¹⁶Institute of High Energy Physics, Vienna 1050¹⁷Institute for High Energy Physics, Protvino 142281¹⁸INFN - Sezione di Torino, 10125 Torino¹⁹Institute for Theoretical and Experimental Physics, Moscow 117218²⁰J. Stefan Institute, 1000 Ljubljana²¹Kanagawa University, Yokohama 221-8686²²Institut für Experimentelle Kernphysik, Karlsruher Institut für Technologie, 76131 Karlsruhe²³Kavli Institute for the Physics and Mathematics of the Universe (WPI), University of Tokyo, Kashiwa 277-8583²⁴Korea Institute of Science and Technology Information, Daejeon 305-806²⁵Korea University, Seoul 136-713²⁶Kyungpook National University, Daegu 702-701²⁷École Polytechnique Fédérale de Lausanne (EPFL), Lausanne 1015²⁸Faculty of Mathematics and Physics, University of Ljubljana, 1000 Ljubljana²⁹University of Maribor, 2000 Maribor³⁰Max-Planck-Institut für Physik, 80805 München

- ³¹*School of Physics, University of Melbourne, Victoria 3010*
³²*Moscow Physical Engineering Institute, Moscow 115409*
³³*Moscow Institute of Physics and Technology, Moscow Region 141700*
³⁴*Graduate School of Science, Nagoya University, Nagoya 464-8602*
³⁵*Kobayashi-Maskawa Institute, Nagoya University, Nagoya 464-8602*
³⁶*Nara Women's University, Nara 630-8506*
³⁷*Department of Physics, National Taiwan University, Taipei 10617*
³⁸*H. Niewodniczanski Institute of Nuclear Physics, Krakow 31-342*
³⁹*Nippon Dental University, Niigata 951-8580*
⁴⁰*Niigata University, Niigata 950-2181*
⁴¹*University of Nova Gorica, 5000 Nova Gorica*
⁴²*Osaka City University, Osaka 558-8585*
⁴³*Pacific Northwest National Laboratory, Richland, Washington 99352*
⁴⁴*Panjab University, Chandigarh 160014*
⁴⁵*Peking University, Beijing 100871*
⁴⁶*Punjab Agricultural University, Ludhiana 141004*
⁴⁷*University of Science and Technology of China, Hefei 230026*
⁴⁸*Soongsil University, Seoul 156-743*
⁴⁹*Sungkyunkwan University, Suwon 440-746*
⁵⁰*School of Physics, University of Sydney, New South Wales 2006*
⁵¹*Department of Physics, Faculty of Science, University of Tabuk, Tabuk 71451*
⁵²*Tata Institute of Fundamental Research, Mumbai 400005*
⁵³*Excellence Cluster Universe, Technische Universität München, 85748 Garching*
⁵⁴*Toho University, Funabashi 274-8510*
⁵⁵*Tohoku Gakuin University, Tagajo 985-8537*
⁵⁶*Tohoku University, Sendai 980-8578*
⁵⁷*Department of Physics, University of Tokyo, Tokyo 113-0033*
⁵⁸*Tokyo Institute of Technology, Tokyo 152-8550*
⁵⁹*Tokyo Metropolitan University, Tokyo 192-0397*
⁶⁰*Tokyo University of Agriculture and Technology, Tokyo 184-8588*
⁶¹*CNP, Virginia Polytechnic Institute and State University, Blacksburg, Virginia 24061*
⁶²*Wayne State University, Detroit, Michigan 48202*
⁶³*Yamagata University, Yamagata 990-8560*
⁶⁴*Yonsei University, Seoul 120-749*
⁶⁵*Luther College, Decorah, Iowa 52101*
⁶⁶*National United University, Miao Li 36003*
(Received 7 April 2014; published 29 May 2014)

We search for CP violation in neutral charm meson decays using a data sample with an integrated luminosity of 966 fb^{-1} collected with the Belle detector at the KEKB e^+e^- asymmetric-energy collider. The asymmetry obtained in the rate of D^0 and \bar{D}^0 decays to the $\pi^0\pi^0$ final state, $[-0.03 \pm 0.64(\text{stat}) \pm 0.10(\text{syst})]\%$, is consistent with no CP violation. This constitutes an order of magnitude improvement over the existing result. We also present an updated measurement of the CP asymmetry in the $D^0 \rightarrow K_S^0\pi^0$ decay: $A_{CP}(D^0 \rightarrow K_S^0\pi^0) = [-0.21 \pm 0.16(\text{stat}) \pm 0.07(\text{syst})]\%$.

DOI: 10.1103/PhysRevLett.112.211601

PACS numbers: 11.30.Er, 13.25.Ft, 14.40.Lb

Within the standard model (SM), CP violation in charm decays [1–3] is expected to be very small and thus challenging to observe experimentally. Observing such CP violation could indicate new physics. The $D^0 \rightarrow \pi^0\pi^0$ decay proceeds via a singly Cabibbo-suppressed (SCS) amplitude, which is expected to have enhanced interference with new physics amplitudes. Such interference could generate a large CP violation effect. An early observation by LHCb [4] suggested a 3.5 standard deviation (σ) effect on the difference of direct CP asymmetries (ΔA_{CP}) between $D^0 \rightarrow K^+K^-$ and $D^0 \rightarrow \pi^+\pi^-$ decays that was later supported by the CDF experiment [5]. At the end of 2012, the

world average [6] for ΔA_{CP} was 4.6σ away from zero. This triggered much theoretical activity [7] in an attempt to explain the effect.

In the SM, CP violation in SCS charm decays arises due to interference between the tree and loop (penguin) amplitudes and is suppressed by $O(V_{cb}V_{ub}/V_{cs}V_{us}) \sim 10^{-3}$, where V_{ij} are the elements of the Cabibbo-Kobayashi-Maskawa matrix [8]. The uncertainties on these order-of-magnitude estimates are, however, large [3]. Although a large ΔA_{CP} could be explained by non-SM physics, it may be simply due to an unexpectedly enhanced CP -violating SM $c \rightarrow u$ penguin amplitude. In the latter case, one expects

fractional-percent CP asymmetries in other SCS two-body decays such as $D^0 \rightarrow \pi^0 \pi^0$ [9–12]. Recently, new measurements of ΔA_{CP} have been performed [13,14], and the current world average is 2.3σ away from zero [6]. The only search for CP violation in $D^0 \rightarrow \pi^0 \pi^0$ was performed by the CLEO Collaboration using 13.7 fb^{-1} of data [15]; the result was $A_{CP} = (+0.1 \pm 4.8)\%$.

In this Letter, we measure the time-integrated CP -violating asymmetry (A_{CP}) in neutral charm meson decays to a pair of neutral pions, $D^0 \rightarrow \pi^0 \pi^0$ [16]. We also update our $D^0 \rightarrow K_S^0 \pi^0$ result [17] using Belle’s full data sample. The SM predicts a nonzero CP asymmetry in final states containing a neutral kaon due to K^0 - \bar{K}^0 mixing, even if no CP -violating phase exists in the charm decay amplitudes. The expected magnitude for this type of asymmetry is $A_{CP}^{K^0} = (-0.339 \pm 0.007)\%$ [18].

The charge of the accompanying low-momentum or “slow” pion π_s^\pm in the decay $D^{*+} \rightarrow D^0 \pi_s^\pm$ [16] identifies the flavor of the neutral charm meson (whether it is a D^0 or a \bar{D}^0) at its production. The measured asymmetry

$$A_{\text{rec}} = \frac{N_{\text{rec}}^{D^{*+} \rightarrow D^0 \pi_s^+} - N_{\text{rec}}^{D^{*-} \rightarrow \bar{D}^0 \pi_s^-}}{N_{\text{rec}}^{D^{*+} \rightarrow D^0 \pi_s^+} + N_{\text{rec}}^{D^{*-} \rightarrow \bar{D}^0 \pi_s^-}}, \quad (1)$$

where N_{rec} is the number of reconstructed signal events, includes three contributions: the underlying CP asymmetry A_{CP} , the forward-backward asymmetry (A_{FB}) due to γ - Z^0 interference in $e^+e^- \rightarrow c\bar{c}$ and higher-order QED effects [19], and the detection asymmetry between positively and negatively charged pions ($A_{\pi_s^\pm}$). The last contribution depends on the transverse momentum $p_T^{\pi_s}$ and polar angle θ^{π_s} of the slow pion and is independent of the D^0 decay final state. To estimate $A_{\pi_s^\pm}$, we use the Cabibbo-favored decay $D^0 \rightarrow K^- \pi^+$ (“untagged”) and $D^{*+} \rightarrow D^0 \pi_s^+ \rightarrow K^- \pi^+ \pi_s^+$ (“tagged”), and we assume the same A_{FB} for D^{*+} and D^0 mesons [20]. By subtracting the measured asymmetries in these two decay modes, we directly obtain the $A_{\pi_s^\pm}$ correction factor [$O(0.1\%)$]. After A_{rec} is corrected for $A_{\pi_s^\pm}$, one is left with

$$A_{\text{rec}}^{\text{cor}} = A_{CP} + A_{\text{FB}}(\cos \theta^*). \quad (2)$$

While A_{CP} is independent of all kinematic variables, A_{FB} is an odd function of the cosine of the D^{*+} polar angle θ^* in the center of mass (c.m.) system. We thus extract A_{CP} and A_{FB} using

$$A_{CP} = [A_{\text{rec}}^{\text{cor}}(\cos \theta^*) + A_{\text{rec}}^{\text{cor}}(-\cos \theta^*)]/2, \quad (3)$$

and

$$A_{\text{FB}} = [A_{\text{rec}}^{\text{cor}}(\cos \theta^*) - A_{\text{rec}}^{\text{cor}}(-\cos \theta^*)]/2. \quad (4)$$

The analysis is based on a data sample corresponding to an integrated luminosity of 966 fb^{-1} collected at the $\Upsilon(nS)$

resonances ($n = 1, 2, 3, 4, 5$) or 60 MeV below the $\Upsilon(4S)$ resonance with the Belle detector [21] at the KEKB asymmetric-energy e^+e^- collider [22]. In the following, the samples taken at or below the $\Upsilon(4S)$ resonance will be referred to as $\Upsilon(4S)$, while the sample recorded at the $\Upsilon(5S)$ is considered separately. The detector components relevant for our study are a tracking system comprising a silicon vertex detector (SVD) and a 50-layer central drift chamber (CDC), a particle identification (PID) system that consists of a barrel-like arrangement of time-of-flight scintillation counters (TOF) and an array of aerogel threshold Cherenkov counters (ACC), and a CsI(Tl) crystal-based electromagnetic calorimeter (ECL). All these components are located inside a superconducting solenoid coil that provides a 1.5 T magnetic field.

We use Monte Carlo (MC) simulated events representing a luminosity 6 times that of the data to devise selection criteria and investigate possible sources of background. The selection optimization is performed by minimizing the expected statistical error on A_{rec} , where the branching fraction of $D^0 \rightarrow \pi^0 \pi^0$ is set to 8×10^{-4} [23] in MC simulations. The level of background is obtained by appropriately scaling the number of events observed in a data sideband of the reconstructed D^* mass.

Candidates for the $K_S^0 \rightarrow \pi^+ \pi^-$ decay are formed from pairs of oppositely charged tracks having a reconstructed invariant mass within $9 \text{ MeV}/c^2$ (about 3 times the experimental resolution) of the nominal K_S^0 mass [24]. The K_S^0 candidates are also required to satisfy the criteria described in Ref. [25] to ensure that their decay vertices are displaced from the interaction point (IP). We reconstruct neutral pion candidates from pairs of electromagnetic showers in the ECL that are not matched to any charged track. Showers in the barrel (end-cap) region of the ECL must exceed 60 (100) MeV to be considered as a π^0 daughter candidate. The invariant mass of the π^0 candidate must lie within $25 \text{ MeV}/c^2$ (about 4 times the experimental resolution) of the known π^0 mass [24]. The π^0 momentum is required to be greater than 640 (540) MeV/c for the data sample taken at the $\Upsilon(4S)$ ($\Upsilon(5S)$) resonance.

Reconstructed π^0 and K_S^0 candidates are kinematically constrained to the nominal π^0 and K_S^0 mass values and combined to form $D^0 \rightarrow K_S^0 \pi^0$ and $D^0 \rightarrow \pi^0 \pi^0$ candidates. For the former, we retain the D^0 candidates having an invariant mass in the range $1.750 < M < 1.950 \text{ GeV}/c^2$, whereas for the latter the range is $1.758 < M < 1.930 \text{ GeV}/c^2$ in order to suppress background from $D^0 \rightarrow K_S^0(\pi^0 \pi^0)\pi^0$.

We require π_s^\pm candidates to originate from near the IP by restricting their impact parameters along and perpendicular to the z axis to be less than 3 and 1 cm, respectively. The z axis is defined to be the direction opposite the e^+ beam. We do not impose any requirement on the number of SVD hits but require that the ratio of PID likelihoods, $\mathcal{L}_\pi/(\mathcal{L}_\pi + \mathcal{L}_K)$, be greater than 0.4. Here, \mathcal{L}_π

(\mathcal{L}_K) is the likelihood of a track being a pion (kaon) and is calculated using specific ionization from the CDC, time-of-flight information from the TOF, and the number of photoelectrons in the ACC. With the above PID requirement, the pion identification efficiency is above 95% with a kaon misidentification probability below 5%.

D^{*+} candidates are reconstructed by combining the π_s^+ with a D^0 candidate and requiring that the resultant ΔM value lies in the range $[0.14, 0.16]$ GeV/c^2 , where $\Delta M \equiv M(D^{*+}) - M(D^0)$. In order to improve the ΔM resolution, the π_s^+ is constrained to originate from the IP. The sideband used for the selection optimization is $0.15 < \Delta M < 0.16$ GeV/c^2 . D mesons produced in B meson decays are rejected by requiring that the D^{*+} candidates have a c.m. momentum greater than 2.5 and 3.1 GeV/c , respectively, for data taken near the $\Upsilon(4S)$ and $\Upsilon(5S)$ resonance. This requirement also significantly reduces combinatorial background.

After applying all selection criteria, we find that about 6% of the total $D^* \rightarrow D(\pi^0\pi^0)\pi_s$ events contain multiple candidates, of which about half are due to a misreconstructed π^0 and about half due to a misreconstructed π_s . We select a single D^0 candidate per event by choosing that which has the smallest χ_{BCS}^2 . This quantity is defined as

$$\chi_{\text{BCS}}^2 = \sum \chi_{\pi^0}^2 + \left[\frac{M(D^0) - m_{D^0}}{\sigma_M} \right]^2, \quad (5)$$

where $\chi_{\pi^0}^2$ is the π^0 mass-constrained fit statistic, σ_M is the uncertainty on the reconstructed D mass as determined from MC simulations, and m_{D^0} is the nominal D^0 mass [24]. In case the D^0 candidate is common to more than one D^* candidate, we select the one having the slow pion with the smallest impact parameter perpendicular to the z axis. According to MC simulation, this procedure identifies the correct D^* candidate among multiple candidates about 74% of the time.

Figure 1 shows the ΔM distributions of event candidates in the two decay modes. We describe the signal shapes by the sum of symmetric and asymmetric Gaussian functions with a common mean. The background shapes are modeled with a threshold function as $(x - m_\pi)^\alpha \exp[-\beta(x - m_\pi)]$, where m_π is the nominal charged pion mass [24] and α and β are shape parameters. The asymmetry A_{rec} and the sum of the D^{*+} and D^{*-} yields are obtained from a simultaneous fit to their ΔM distributions. The parameters common in the fit are (for signal) the common mean, the widths of the symmetric and the asymmetric Gaussian functions, and the relative fraction of the two functions, (for background) α and β . The signal yield for $D^0 \rightarrow \pi^0\pi^0$ is 34460 ± 273 events and $A_{\text{rec}} = (+0.29 \pm 0.64)\%$. For the $D^0 \rightarrow K_S^0\pi^0$ case, the signal yield is 466814 ± 773 events and $A_{\text{rec}} = (+0.29 \pm 0.15)\%$.

The data samples shown in Fig. 1 are divided into ten bins of $\cos\theta^*$, seven bins of $p_T^{\pi_s}$, and eight bins of $\cos\theta^{\pi_s}$. For each 3D bin, a simultaneous fit analogous to the one

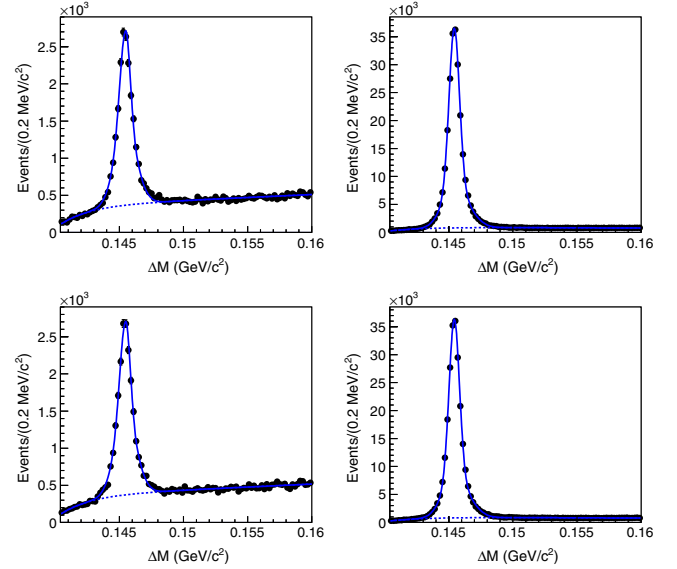


FIG. 1 (color online). Distributions of the mass difference ΔM for the $\pi^0\pi^0$ (left) and $K_S^0\pi^0$ (right) final states. Top (bottom) plots are for the D^{*+} (D^{*-}) sample. Points with error bars are the data, the solid curves show the results of the fit, and the dashed curves are the background predictions.

used for the full sample is performed, and the asymmetry obtained for each bin is corrected by the corresponding $A_{\pi_s}^{\pi_s}$ obtained in Ref. [17]. Because of limited statistics, the shape for the $D^0 \rightarrow \pi^0\pi^0$ signal in a bin of $[p_T^{\pi_s}, \cos\theta^{\pi_s}]$ is taken from the larger $K_S^0\pi^0$ sample. We account for small differences between the two samples using MC simulations. Bins with fewer than 30 events, which correspond to only 2% of the total statistics in the $D^0 \rightarrow \pi^0\pi^0$ sample, are removed from the A_{CP} estimation. A weighted average over the $[p_T^{\pi_s}, \cos\theta^{\pi_s}]$ bins having the same $\cos\theta^*$ value is then performed, and A_{CP} and A_{FB} are extracted from Eqs. (3) and (4), respectively. This procedure has been verified with six sets of generic MC samples, each of similar size as the data; the resulting A_{CP} values were found to be in agreement with the generated values. Figure 2 shows A_{CP} and A_{FB} as a function of $|\cos\theta^*|$ obtained for the two data samples. From the weighted average over the $|\cos\theta^*|$ bins, we obtain

$$A_{CP}(\pi^0\pi^0) = (-0.03 \pm 0.64)\%, \quad (6)$$

$$A_{CP}(K_S^0\pi^0) = (-0.10 \pm 0.16)\%, \quad (7)$$

where the uncertainties are statistical only, with a reduced χ^2 of 1.7 and 0.7, respectively. The observed A_{FB} values decrease with $|\cos\theta^*|$ as expected but are somewhat lower than the leading-order QED prediction [19]. Higher-order corrections are expected to lower the theoretical prediction, which would bring it into better agreement with our data.

We identify three significant sources of systematic uncertainty (see Table I). The first is due to the uncertainty

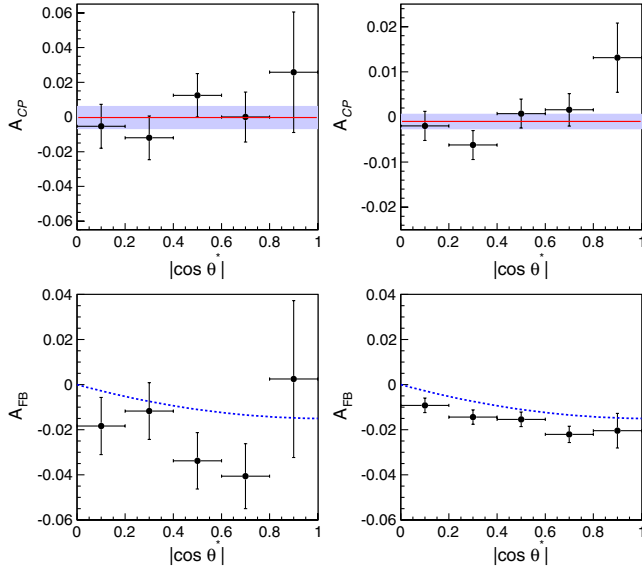


FIG. 2 (color online). CP violation asymmetry A_{CP} (top) and forward-backward asymmetry A_{FB} (bottom) values as a function of $|\cos \theta^*|$. Plots on the left (right) are for the $\pi^0 \pi^0$ ($K_S^0 \pi^0$) final state. The solid red lines represent the central values obtained from a least-squares minimization, the blue regions for the A_{CP} plots show the 1σ interval, and the dashed blue curves for the A_{FB} plots show the leading-order prediction for $A_{FB}(e^+e^- \rightarrow c\bar{c})$.

in the signal shapes, which, in the case of $D^0 \rightarrow \pi^0 \pi^0$, is dominated by the statistics of the calibration mode $D^0 \rightarrow K_S^0 \pi^0$. The second is the slow pion efficiency correction. We estimate its contribution by varying $A_{e^{\pi_s}}$ by its statistical error in each of the 7×8 bins of $[p_T^{\pi_s}, \cos \theta^{\pi_s}]$. The third is the A_{CP} extraction procedure itself and is obtained by varying the binning in $|\cos \theta^*|$. For the $D^0 \rightarrow K_S^0 \pi^0$ channel, we correct for a nonvanishing asymmetry originating from the different strong interaction of K^0 and \bar{K}^0 mesons with nucleons of the detector material, estimated to be -0.11% in Ref. [26], and assign an additional systematic uncertainty of 0.01% . Finally, we add these individual contributions in quadrature to obtain the total systematic uncertainty. The result is 0.10% (0.07%) for the $\pi^0 \pi^0$ ($K_S^0 \pi^0$) sample.

In summary, we have measured the time-integrated CP -violating asymmetry A_{CP} in the $D^0 \rightarrow \pi^0 \pi^0$ decay using 966 fb^{-1} of data. After correcting for the detector-induced asymmetries with a precision of 0.07% by using the tagged and untagged $D^0 \rightarrow K^- \pi^+$ decays, we obtain

TABLE I. Summary of systematic uncertainties (%) in A_{CP} .

Source	$\pi^0 \pi^0$	$K_S^0 \pi^0$
Signal shape	± 0.03	± 0.01
Slow pion correction	± 0.07	± 0.07
A_{CP} extraction method	± 0.07	± 0.02
K^0/\bar{K}^0 -material effects	\dots	± 0.01
Total	± 0.10	± 0.07

$$A_{CP}(D^0 \rightarrow \pi^0 \pi^0) = (-0.03 \pm 0.64 \pm 0.10)\%, \quad (8)$$

where the uncertainties are statistical and systematic, respectively. The measured CP asymmetry has an order of magnitude better precision than the previous result [15] and shows no evidence for CP violation. We also measure

$$A_{CP}(D^0 \rightarrow K_S^0 \pi^0) = (-0.21 \pm 0.16 \pm 0.07)\%, \quad (9)$$

which supersedes our earlier result [17]. After subtracting CP violation due to K^0 - \bar{K}^0 mixing, $(-0.339 \pm 0.007)\%$ [18], the CP asymmetry in $D^0 \rightarrow \bar{K}^0 \pi^0$ decay is found to be $(+0.12 \pm 0.16 \pm 0.07)\%$, which is consistent with no CP violation.

We thank the KEKB group for excellent operation of the accelerator, the KEK cryogenics group for efficient solenoid operations, and the KEK computer group, the NII, and PNNL/EMSL for valuable computing and SINET4 network support. We acknowledge support from MEXT, JSPS and Nagoya's TLPRC (Japan); ARC and DIISR (Australia); FWF (Austria); NSFC (China); MSMT (Czechia); CZF, DFG, and VS (Germany); DST (India); INFN (Italy); MOE, MSIP, NRF, GSDC of KISTI, BK21Plus, and WCU (Korea); MNiSW and NCN (Poland); MES and RFAAE (Russia); ARRS (Slovenia); IKERBASQUE and UPV/EHU (Spain); SNSF (Switzerland); NSC and MOE (Taiwan); and DOE and NSF (U.S.).

- [1] I. I. Bigi, A. Paul, and S. Recksiegel, *J. High Energy Phys.* **06** (2011) 089.
- [2] G. Isidori, J. F. Kamenik, Z. Ligeti, and G. Perez, *Phys. Lett. B* **711**, 46 (2012).
- [3] J. Brod, A. L. Kagan, and J. Zupan, *Phys. Rev. D* **86**, 014023 (2012).
- [4] R. Aaij *et al.* (LHCb Collaboration), *Phys. Rev. Lett.* **108**, 111602 (2012).
- [5] T. Aaltonen *et al.* (CDF Collaboration), *Phys. Rev. Lett.* **109**, 111801 (2012).
- [6] Y. Amhis *et al.* (Heavy Flavor Averaging Group), [arXiv:1207.1158](http://arxiv.org/abs/1207.1158); updates available at <http://www.slac.stanford.edu/xorg/hfag>.
- [7] A. Lenz, [arXiv:1311.6447](http://arxiv.org/abs/1311.6447), and references within.
- [8] N. Cabibbo, *Phys. Rev. Lett.* **10**, 531 (1963); M. Kobayashi and T. Maskawa, *Prog. Theor. Phys.* **49**, 652 (1973).
- [9] H.-Y. Cheng and C.-W. Chiang, *Phys. Rev. D* **85**, 034036 (2012); **85**, 079903(E) (2012); **86**, 014014 (2012).
- [10] B. Bhattacharya, M. Gronau, and J. L. Rosner, *Phys. Rev. D* **85**, 054014 (2012).
- [11] Y. Grossman, A. L. Kagan, and J. Zupan, *Phys. Rev. D* **85**, 114036 (2012).
- [12] G. Hiller, M. Jung, and S. Schacht, *Phys. Rev. D* **87**, 014024 (2013).
- [13] (LHCb Collaboration), LHCb-CONF-2013-003.
- [14] R. Aaij *et al.* (LHCb Collaboration), *Phys. Lett. B* **723**, 33 (2013).

- [15] G. Bonvicini *et al.* (CLEO Collaboration), *Phys. Rev. D* **63**, 071101 (2001).
- [16] Throughout this Letter, the charge-conjugate decay mode is implied unless stated otherwise.
- [17] B. R. Ko *et al.* (Belle Collaboration), *Phys. Rev. Lett.* **106**, 211801 (2011).
- [18] B. R. Ko *et al.* (Belle Collaboration), *Phys. Rev. Lett.* **109**, 021601 (2012); **109**, 1199039(E) (2012).
- [19] F. A. Berends, K. J. F. Gaemers, and R. Gastmans, *Nucl. Phys.* **B63**, 381 (1973); R. W. Brown, K. O. Mikaelian, V. K. Cung, and E. A. Paschos, *Phys. Lett.* **43B**, 403 (1973); R. J. Cashmore, C. M. Hawkes, B. W. Lynn, and R. G. Stuart, *Z. Phys. C* **30**, 125 (1986).
- [20] M. Staric *et al.* (Belle Collaboration), *Phys. Lett. B* **670**, 190 (2008).
- [21] A. Abashian *et al.* (Belle Collaboration), *Nucl. Instrum. Methods Phys. Res., Sect. A* **479**, 117 (2002); also, see the detector section in J. Brodzicka *et al.*, *Prog. Theor. Exp. Phys.*, 04D001 (2012).
- [22] S. Kurokawa and E. Kikutani, *Nucl. Instrum. Methods Phys. Res., Sect. A* **499**, 1 (2003), and other papers in this volume; T. Abe *et al.*, *Prog. Theor. Exp. Phys.*, 03A001 (2013), and following articles up to 03A011.
- [23] J. P. Lees *et al.* (BABAR Collaboration), *Phys. Rev. D* **85**, 091107 (2012).
- [24] J. Beringer *et al.* (Particle Data Group), *Phys. Rev. D* **86**, 010001 (2012).
- [25] K.-F. Chen *et al.* (Belle Collaboration), *Phys. Rev. D* **72**, 012004 (2005).
- [26] B. R. Ko, E. Won, B. Golob, and P. Pakhlov, *Phys. Rev. D* **84**, 111501 (2011).